Overcoming the Cystic Fibrosis Sputum Barrier to Leading Adeno-associated Virus Gene Therapy Vectors

Benjamin S Schuster[1,2], Anthony J Kim[2,9], Joshua C Kays[1,2], Mia M Kanzawa[1,2], William B Guggino[3], Michael P Boyle[4], Steven M Rowe[5], Nicholas Muzyczka[6], Jung Soo Suk[2,7] and Justin Hanes[1,2,7,8]

[1]Department of Biomedical Engineering, Johns Hopkins University School of Medicine, Baltimore, Maryland, USA; [2]Center for Nanomedicine, Johns Hopkins University School of Medicine, Baltimore, Maryland, USA; [3]Department of Physiology, Johns Hopkins University School of Medicine, Baltimore, Maryland, USA; [4]Division of Pulmonary and Critical Care Medicine, Johns Hopkins Adult Cystic Fibrosis Program, Johns Hopkins University School of Medicine, Baltimore, Maryland, USA; [5]Department of Medicine, University of Alabama at Birmingham, Birmingham, Alabama, USA; [6]Department of Molecular Genetics and Microbiology, and Powell Gene Therapy Center, University of Florida College of Medicine, Gainesville, Florida, USA; [7]Department of Ophthalmology, Johns Hopkins University School of Medicine, Baltimore, Maryland, USA; [8]Institute for NanoBioTechnology, Johns Hopkins University, Baltimore, Maryland, USA; [9]Current address: Departments of Neurosurgery and Pharmaceutical Sciences, University of Maryland, Baltimore, Baltimore, Maryland, USA

Gene therapy has not yet improved cystic fibrosis (CF) patient lung function in human trials, despite promising preclinical studies. In the human CF lung, inhaled gene vectors must penetrate the viscoelastic secretions coating the airways to reach target cells in the underlying epithelium. We investigated whether CF sputum acts as a barrier to leading adeno-associated virus (AAV) gene vectors, including AAV2, the only serotype tested in CF clinical trials, and AAV1, a leading candidate for future trials. Using multiple particle tracking, we found that sputum strongly impeded diffusion of AAV, regardless of serotype, by adhesive interactions and steric obstruction. Approximately 50% of AAV vectors diffused >1,000-fold more slowly in sputum than in water, with large patient-to-patient variation. We thus tested two strategies to improve AAV diffusion in sputum. We showed that an AAV2 mutant engineered to have reduced heparin binding diffused twice as fast as AAV2 on average, presumably because of reduced adhesion to sputum. We also discovered that the mucolytic *N*-acetylcysteine could markedly enhance AAV diffusion by altering the sputum microstructure. These studies underscore that sputum is a major barrier to CF gene delivery, and offer strategies for increasing AAV penetration through sputum to improve clinical outcomes.

Received 6 March 2014; accepted 14 May 2014; advance online publication 24 June 2014. doi:10.1038/mt.2014.89

INTRODUCTION

Cystic fibrosis (CF) is an autosomal recessive disorder that afflicts ~70,000 people worldwide.[1] In patients with CF, absence of functional CF transmembrane conductance regulator (CFTR), a chloride channel, impairs salt and water balance at epithelial surfaces.[2] Lung disease is the primary cause of morbidity and mortality in CF. A vicious cycle of airway obstruction, infection, and inflammation causes progressive decline in patient lung function.[2,3] The median predicted survival age of CF patients has climbed in recent decades, thanks to new drugs, early diagnosis, and improved care, but it is still only about 40 years.[2]

After the discovery of the *CFTR* gene in 1989, researchers envisioned treating CF by delivering the correct gene directly to patient lungs to restore CFTR function.[3] In cell culture and animal models, gene therapy has successfully mediated CFTR expression and corrected chloride current.[4,5] However, achieving clinical efficacy in humans has proved challenging.[3,6] Despite 25 clinical trials testing adenovirus (AdV), adeno-associated virus (AAV), and nonviral vectors, gene therapy has yet to produce clinically significant improvements in CF patient lung function.[3,6] These disappointing results have been blamed on immune response to the gene vectors, inefficient transduction of human airway epithelium via the apical membrane, and weak promoters to drive gene expression.[7]

Another major obstacle to pulmonary gene therapy for CF is the layer of viscoelastic airway secretions that coats the CF lung epithelium.[3,7,8] CF airway secretions are a gel comprised of entangled and crosslinked mucins, DNA, actin, and other macromolecules and cell debris.[9] This biopolymer network may trap inhaled particles by steric obstruction and specific or nonspecific adhesive interactions.[7,10] Nevertheless, most CF gene therapy preclinical research has been conducted using cell culture and animal models that lack CF-like airway secretions and thus do not fully mimic the CF lung.[3] We previously found, in a proof-of-concept study, that sputum from five CF patients strongly hindered diffusion of AdV and AAV serotype 5 (AAV5).[11] Likewise, CF sputum inhibited AdV-mediated transfection in *in vitro* and *ex vivo* experiments.[12] These studies underscore that airway secretions can act as a barrier and prevent inhaled viral vectors from reaching target lung cells.

Given its clinical significance, much remains to be learned about the CF sputum barrier to AAV gene therapy. AAV2 was

Correspondence: Justin Hanes, Center for Nanomedicine, Johns Hopkins University School of Medicine, 400 N. Broadway, Robert H. and Clarice Smith Building, 6th Floor, Baltimore, Maryland 21231, USA. E-mail: hanes@jhmi.edu

the first AAV serotype characterized and the only one tested in CF clinical trials, yet whether AAV2 can penetrate CF sputum is unknown. AAV is a leading viral gene delivery platform, and numerous other AAV serotypes have been investigated for their ability to transduce airway cells.[8,13] AAV5 exhibited enhanced transduction efficiency in the mouse lung compared with AAV2,[13] which motivated our prior work testing AAV5 diffusion in CF sputum.[11] A more recent study showed that AAV1 outperforms AAV5 in human primary airway cells and in chimpanzees.[8] Because AAV1 has emerged as a promising candidate for future CF gene therapy clinical trials, its ability to penetrate CF sputum must also be assessed. All AAV serotypes have nonenveloped, icosahedral, ~25-nm-diameter capsids,[14] so the sputum mesh will sterically obstruct all serotypes equally. However, the serotypes differ in their tropisms and binding affinities,[14–17] which may alter their adhesion to, and thus their diffusion through, sputum.

Here, we investigated diffusion of AAV1 and AAV2, compared with AAV5, in sputum samples from adult CF patients. Using multiple particle tracking and automated image analysis, we measured the movement of >30,000 AAV particles at single virus resolution in >20 patient samples. We observed that CF sputum hindered a large fraction of AAV particles, regardless of serotype. The sizeable patient population and the number of viruses studied enabled us to examine inter- and intrapatient variability. Furthermore, we demonstrated two methods to improve AAV diffusion in CF sputum: virus capsid modification and mucolytic therapy with *N*-acetylcysteine. Our findings suggest strategies and future research directions for overcoming the CF sputum barrier to clinically successful inhaled gene delivery.

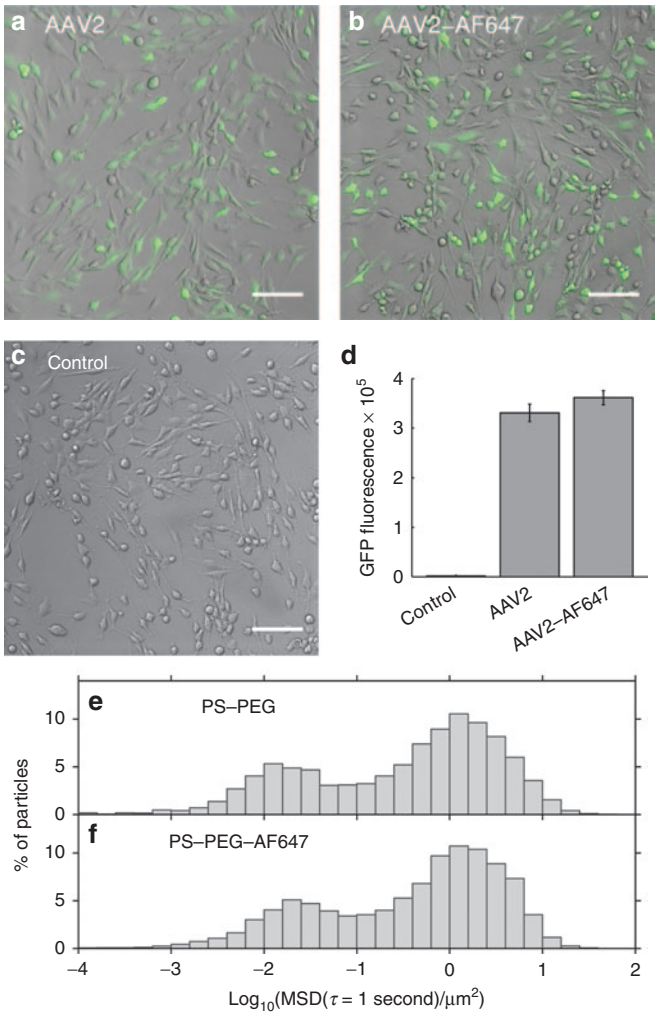

Figure 1 Effect of AlexaFluor 647 (AF647) dye labeling on adeno-associated virus (AAV) transduction in BEAS-2B cells and on nanoparticle transport in cystic fibrosis (CF) sputum. (**a–d**) BEAS-2B cells transduced (**a**) with AAV2 or (**b**) with AF647-labeled AAV2 (AAV2-AF647) are compared with (**c**) untreated control cells. The AAV packaged a green fluorescent protein (GFP) reporter gene; green indicates GFP expression. Scale bars represent 100 μm. (**d**) Flow cytometry comparing GFP expression in BEAS-2B cells transduced with AAV2 versus AAV2-AF647. Results shown are mean cell fluorescence, in arbitrary units. Error bars denote standard error of the mean ($n = 3$). The difference in transduction between AAV2 and AAV2-AF647 is not statistically significant. (**e–f**) Multiple particle tracking in CF sputum samples of (**e**) 100-nm PS-PEG particles versus (**f**) 100-nm PS-PEG particles labeled with AF647 (PS-PEG-AF647). Graphs show distribution of individual particles' mean squared displacement (MSD) at a time scale of 1 second. Data represent six sputum samples, with an average of >1500 particles of each type tracked per sample.

RESULTS

Characterization of fluorescently labeled AAV

We labeled the AAV capsid with a deep red fluorescent dye, Alexa Fluor 647 (AF647), to track the movement of AAV in freshly collected human CF sputum. To assess whether attaching this exogenous dye molecule would affect our subsequent studies, we examined the consequences of dye labeling on AAV infectivity and on particle transport in CF sputum.

First, we examined whether AF647 labeling altered AAV infectivity. We infected BEAS-2B bronchial epithelial cells with AAV2 or with AF647-labeled AAV2 (AAV2-AF647) at the same multiplicity of infection. The virus carried a green fluorescent protein (GFP) reporter gene, which allowed us to assess transduction efficiency by fluorescence microscopy and flow cytometry (**Figure 1a–d**). We found no statistically significant difference in gene expression by the cells infected with AAV2 compared with infection with AAV2-AF647 (two-sided *t*-test, $P = 0.25$). Next, we examined whether attaching AF647 affected particle diffusion in CF sputum. Since we could not image unlabeled AAV, we addressed this question using polystyrene (PS) nanoparticles

Table 1 Hydrodynamic diameter (nm) of unlabeled versus Alexa Fluor-labeled AAV and PS-PEG particles

	Unlabeled[a]	Labeled[a,b]
AAV1	20 ± 1	19 ± 1
AAV2	30 ± 1	30 ± 1
AAV5	21 ± 1	19 ± 1
AAV2 mutant	28 ± 0.2	28 ± 1
PS-PEG	128 ± 5	125 ± 1

AAV, adeno-associated virus; PS-PEG, polystyrene particles coated with polyethylene glycol

[a]Measured by dynamic light scattering (DLS), using a Malvern Zetasizer Nano ZS. Data represent the mean of $n = 3$ measurements. Error values represent standard deviation. [b]For these measurements, AAV was labeled with Alexa Fluor 555, rather than Alexa Fluor 647 (AF647), which was the dye used for the particle-tracking experiments. The DLS instrument uses a 633-nm laser, so compounds such as AF647 that strongly absorb 633-nm light interfere with the size measurement and are incompatible with the instrument (see Malvern manual).

internally labeled with a fluorescent dye, and which were densely coated with polyethylene glycol (PEG) to minimize adhesion to sputum (PS-PEG).[10,18,19] We measured the transport in CF sputum of 100-nm PS-PEG particles compared with 100-nm PS-PEG particles further labeled with AF647 on the particle surface (PS-PEG-AF647). A histogram of the mean squared displacement (MSD) of PS-PEG particles in CF sputum (**Figure 1e**) was nearly identical to that of PS-PEG-AF647 (**Figure 1f**). Finally, using dynamic light scattering, we confirmed that dye labeling did not affect the size of AAV or PS-PEG particles (**Table 1**). Together, these studies strongly suggest that labeling AAV with dye did not alter its biological activity or diffusivity.

Transport of AAV serotypes 1, 2, and 5 in CF sputum

We studied the diffusion of AAV serotypes 1, 2, and 5, as well as polymeric nanoparticles for comparison, in 10 CF sputum samples. Using particle tracking and automated image analysis, we analyzed the trajectories of tens of thousands of viruses and nanoparticles. Histograms of individual particle MSDs at a time scale of 1 second, averaged over the 10 patient samples with each sample equally weighted, are shown in **Figure 2** and **Supplementary Figure S2**. In 20 °C water, a 25-nm-diameter AAV particle would have a two-dimensional MSD of 69 μm^2 at 1 second, according to Stokes–Einstein theory.[20,21] In comparison, all the three AAV serotypes were greatly slowed in CF sputum (**Figure 2b–d**). Approximately 50% of the AAV particles moved less than 1/1,000th their theoretical MSD in water, with MSD < 0.069 μm^2 (or $\log_{10}$MSD < −1.2) at 1 second.

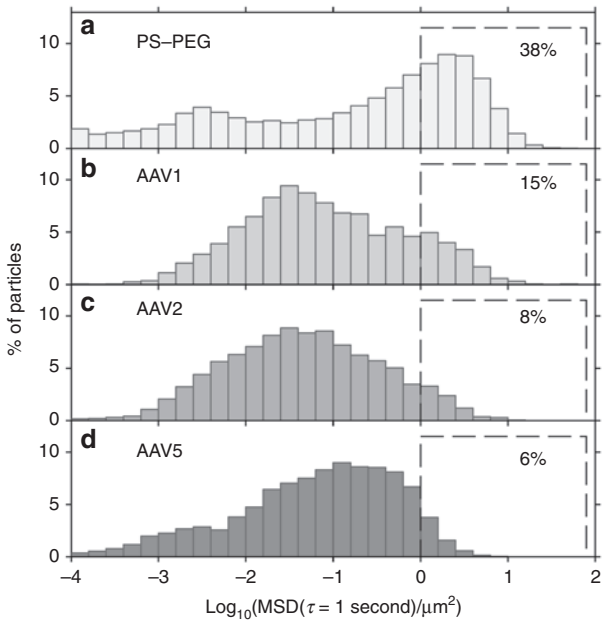

Figure 2 Transport in cystic fibrosis (CF) sputum samples of adeno-associated virus (AAV)1, AAV2, and AAV5, compared with 100-nm PS-PEG control particles. Distribution of individual particle mean squared displacement (MSD) values at a time scale of 1 second for (**a**) 100-nm PS-PEG particles, (**b**) AAV1, (**c**) AAV2, and (**d**) AAV5. Data represent the average of 10 sputum samples, with each sample equally weighted, and with an average of >500 particles of each type tracked per sample. Percentage of particles that moved rapidly, defined as $\log_{10}$MSD ≥ 0 at a time scale of 1 second, is shown for each particle type (dashed boxes).

We found that transport rates of individual particles in sputum ranged as much as five orders of magnitude (**Figures 2** and **3**), compared with approximately three orders of magnitude for AAV in water (**Supplementary Figure S3**), which reflects the heterogeneous nature of CF sputum.[22] Fast-moving particles are of particular interest, since they have the greatest likelihood of penetrating the sputum layer. All the AAV serotypes tested had a subpopulation of fast-moving particles, which we define as those with MSD ≥ 1 μm^2 (or $\log_{10}$MSD ≥ 0) at 1 second. Using this definition for fast-moving particles, it was found that 15, 8, and 6% of AAV1, AAV2, and AAV5, respectively, diffused rapidly in CF sputum (**Figure 2b–d**). The MSDs of these fast particles typically increased linearly with time, so if we extrapolate, a freely diffusing particle that has an MSD (measured by two-dimensional particle tracking) of 1 μm^2 at 1 second could penetrate a 10-μm sputum layer (considering only motion in the z-direction) in 200 seconds. Likewise, the same particle could penetrate a 40-μm sputum layer in about 50 minutes. In other words, the small but important subpopulation of fast-moving particles would be able to traverse physiologically relevant distances[9] in under an hour, and may be more likely to penetrate the airway secretions and reach epithelial cells *in vivo* prior to being removed from the lungs by mucociliary clearance. Measurements of mucociliary clearance rates in CF patients vary widely; the percentage of inhaled particles cleared from CF lungs within an hour ranged from about 15 to 60% in various studies.[23]

Overall, only ~5–15% of AAV particles were diffusive, while the majority of particles were greatly hindered or immobilized in sputum. For comparison, we also measured the diffusion of polymeric nanoparticles in sputum. Our lab has previously shown that small polymeric nanoparticles, if densely coated with PEG to render their surfaces hydrophilic and resistant to mucus adhesion, diffuse faster in sputum than do comparably sized adhesive particles. However, particles larger than the mesh size of the sputum, even if PEG-coated, are sterically immobilized.[10,18] Here, we found that in contrast to AAV, nearly 40% of the muco-inert, 100-nm PS-PEG particles diffused rapidly (**Figure 2a**). Meanwhile, only 3% of the 100-nm uncoated carboxylate PS particles (PS-COOH), and only 1% of the 500-nm PS-PEG particles, diffused rapidly in sputum (**Supplementary Figure S2b,c**), which agrees with our previous findings.[18]

Patient-to-patient variation in AAV transport

We found that AAV and 100-nm PS-PEG particle mobility varied substantially from patient to patient. **Figure 3a** shows boxplots of particle MSDs (at a time scale of 1 second) for sputum samples from 10 CF patients; **Figure 3b** shows representative trajectories of particles in three of those samples. On one end of the spectrum is patient 1, in whose sputum sample the majority of AAV and 100-nm PS-PEG particles were immobilized, as illustrated by their highly constrained trajectories. Toward the other end of the spectrum is patient 9, in whose sputum sample larger fractions of AAV and 100-nm PS-PEG particles were diffusive, as can be seen from their Brownian trajectories (**Figure 3b**). Particle transport in sample 1 was significantly different from that in sample 9 (and also significantly different from that in samples 4, 8, and 10; $P < 0.01$ by

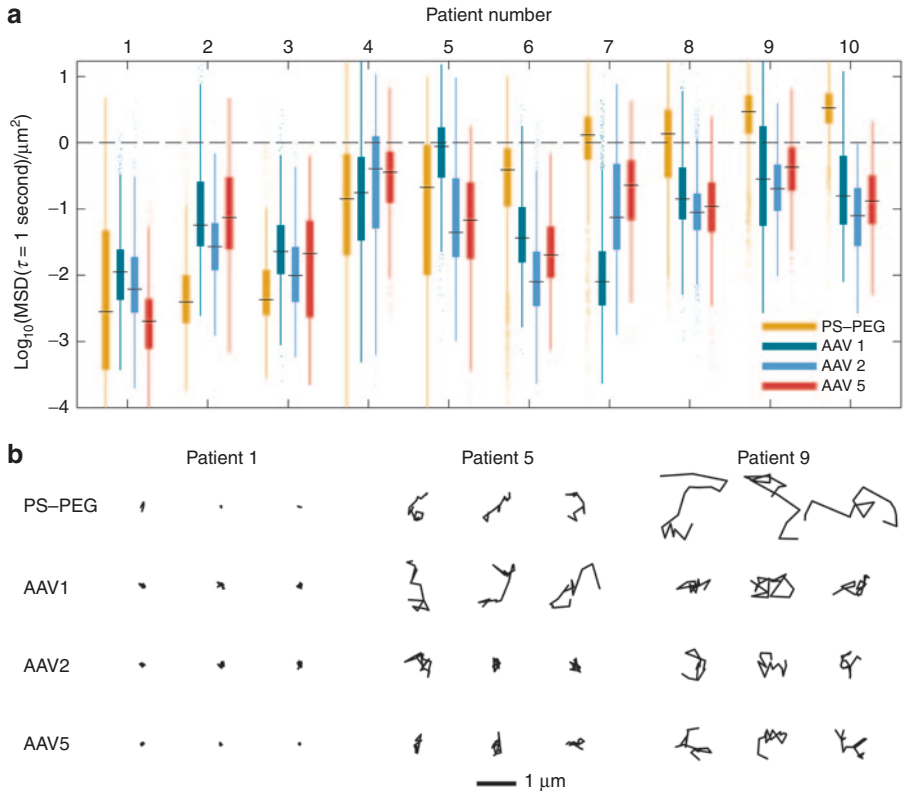

Figure 3 Patient-to-patient variation in adeno-associated virus (AAV) transport. (**a**) Box-and-whisker plots of mean squared displacement (MSD) values (at a time scale of 1 second) of AAV1, AAV2, AAV5, and 100-nm PS-PEG control particles in sputum samples from 10 cystic fibrosis (CF) patients. Maximum whisker length is 1.5 times the interquartile range; outliers are shown as dots. Patients are numbered in ascending order according to the median MSD of 100-nm PS-PEG particles in their sputum sample. The dashed line at $\log_{10}$MSD = 0 is a visual aid to emphasize fast-moving particles, which we define as $\log_{10}$MSD ≥ 0 at a time scale of 1 second. (**b**) Representative trajectories of AAV1, AAV2, AAV5, and 100-nm PS-PEG control nanoparticles in sputum samples from 3 of the aforementioned 10 CF patients. Trajectories show 1 second of motion. The MSDs of the trajectories presented are within the middle 50 percentile for the given patient sample and particle or virus type.

two-way analysis of variance followed by Tukey's honestly significant difference test). The three AAV serotypes tested had similar transport rates within most of the samples. However, in patients 5 and 7, different serotypes exhibited divergent transport behavior. Those sputum samples may have had different binding affinities for different AAV serotypes, but intrasample variability likely also contributed to the variation.

To assess the extent of inter- versus intrasample variability, we tracked 100-nm PS-PEG particles in the same sputum aliquots in which we tracked the various AAV serotypes. This provided us with transport data of one particle type in multiple sputum aliquots from each of nine CF sputum samples (**Supplementary Figure S4**). From these 100-nm PS-PEG particle transport data, we found that the variance between samples of $\log_{10}$MSD was 1.00, which was 50 times the variance within samples, 0.02 (linear mixed-effects model[24] fit by maximum likelihood). This strongly suggests that the variation among different samples can largely be attributed to patient-to-patient differences, rather than to intrasputum sample heterogeneity.

We investigated whether patients' pulmonary function test results (summarized in **Table 2**; higher scores indicate better lung health) could explain the patient-to-patient variation in AAV transport, but we did not find strong correlations. For instance, we found that median $\log_{10}$MSD at 1 second of AAV2 increased marginally with forced expiratory volume (R^2 = 0.33) and forced vital capacity (R^2 = 0.12). Similarly, we found only weak correlations between AAV transport rates and the measured solid content (percent dry weight[10]) of sputum samples (*e.g.*, R^2 = 0.11 for AAV2).

Finally, we note that patients involved in this study received no mucolytics other than Pulmozyme. Furthermore, particle

Table 2 Patient demographics for Figures 2 and 3

Age	31 ± 8
Sex (number of patients)	
M	8
F	2
FEV_1 (% of predicted value)[a]	62 ± 27
FVC (% of predicted value)[b]	83 ± 23
CFTR genotype (number of patients)	
F508del homozygous	7
Other	2
Unknown	1

FEV_1 and FVC are reported as percentages of predicted value for a typical individual. Predicted value is a function of age, sex, and height. Age, FEV_1, and FVC values are mean ± SD.
[a]FEV_1 is forced expiratory volume in 1 second. [b]FVC is forced vital capacity.

transport was not faster in sputum from patients who received Pulmozyme between 2 and 6 hours prior to their sputum sample collection (patients 2 and 5 in **Figure 3**), compared with those who last took Pulmozyme the day before sample collection (patients 1, 3, 7, and 9) and compared with those not on Pulmozyme (patients 4, 6, 8, and 10 in **Figure 3**). This agrees with our prior finding that Pulmozyme treatment of sputum *ex vivo* did not affect particle transport.[25,26] Thus, Pulmozyme treatment status does not appear to be responsible for the patient-to-patient variation in particle transport observed here.

Effect of AAV2 capsid mutation

Adhesion can immobilize particles in sputum, so we next investigated whether modifying the viral capsid to reduce adhesion could improve AAV transport. AAV2 binds to heparan sulfate proteoglycan and heparin.[14] This may pose a challenge for sputum penetration because heparan sulfate is abundant in human tissues and elevated in the CF lung,[27] and has also been identified in sputum from patients with bronchiectasis,[28] a key feature of CF.[2] Thus, we hypothesized that a mutant AAV2, whose capsid was mutated at positions 585 and 588 to reduce heparin binding, as previously described,[14,29,30] would diffuse faster than AAV2 in sputum.

First, to confirm that the AAV2 mutant indeed had reduced binding affinity for heparin, we conducted an *in vitro* heparin competition assay (**Figure 4a**). We added AAV2 or the AAV2 mutant to BEAS-2B bronchial epithelial cells bathed in media with increasing concentrations of dissolved heparin. We assessed transduction efficiency by measuring AAV-mediated GFP expression using flow cytometry. Indeed, heparin inhibited AAV2 transduction significantly more strongly than it inhibited the AAV2 mutant (*t*-test; $P < 0.01$) for each of the three heparin concentrations tested. To check the validity of our assay, we confirmed that heparin did not inhibit BEAS-2B transduction by AAV1 or AAV5, as expected (**Supplementary Figure S5**).

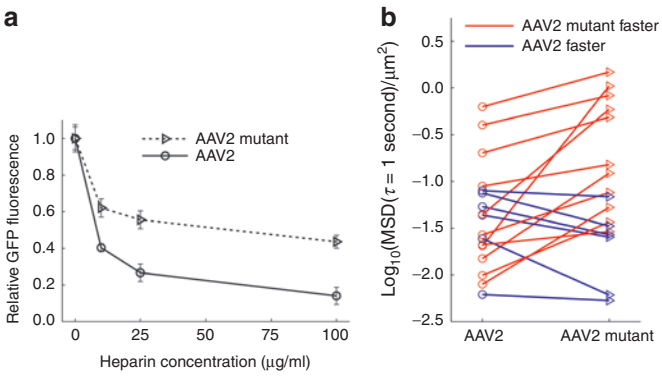

Figure 4 Effect of mutation in adeno-associated virus (AAV)2 heparin-binding domain. (**a**) Effect of soluble heparin on transduction of BEAS-2B cells by AAV2 versus AAV2 mutant, which was engineered to reduce heparin binding. Green fluorescent protein (GFP) expression by transduced cells was measured by flow cytometry. Values shown are relative to GFP expression in the absence of soluble heparin for the respective AAV serotype. Error bars indicate standard error of the mean ($n \geq 3$). Difference is statistically significant ($P < 0.01$) at 10, 25, and 100 μg/ml. (**b**) Transport in 17 cystic fibrosis (CF) sputum samples of AAV2 versus AAV2 mutant. Each marker represents the median mean squared displacement at a timescale of 1 second in one patient sample. Lines connect pairs of data from the same patient's sample. Difference is statistically significant ($P < 0.01$). See methods section for details on statistics.

To study the effect of the capsid mutation on diffusion in sputum, we tracked AAV2 and the AAV2 mutant in sputum samples from 17 patients (**Figure 4b**). We found that the capsid mutation did affect AAV transport ($\chi^2 = 6.86$, $P = 0.0088$), increasing the median MSD at a time scale of 1 s by a factor of 2.2 ± 1.3. In four of the sputum samples, the median MSD of the AAV2 mutant was more than five times that of AAV2. Furthermore, in two sputum samples, there was more than an order of magnitude increase. However, since steric obstruction and adhesion to other sputum components besides heparan can also contribute to hindering AAV motion, we did not observe the largest improvements specifically in samples where AAV2 diffusion was poor. Overall, the data suggest that engineering the AAV2 capsid to reduce its adhesion to heparin can improve AAV2 transport in sputum.

Effect of *N*-acetylcysteine treatment

Previously, our group reported that pretreatment of CF sputum with the mucolytic drug *N*-acetylcysteine (NAC) resulted in improved transport of PS-PEG particles and nonviral gene carriers through the sputum.[25,26] NAC, which is US Food and Drug Administration–approved for various routes of administration, including inhalation, breaks disulfide bonds that crosslink mucins into polymers and thereby reduces sputum viscoelasticity.[7,9] Here, we investigated whether pretreatment of sputum with NAC would also enhance AAV diffusion.

We measured AAV1 diffusion in untreated CF sputum compared with sputum pretreated with 5 mmol/l NAC. We chose this concentration based on our earlier finding that millimolar concentrations of NAC enhanced PS-PEG particle transport in sputum, whereas concentrations one order of magnitude lower were much less effective.[26] NAC solution prescribed for inhalation (Mucomyst) contains a concentration of 1.2 mol/l, or 20%, NAC. Following a single treatment of NAC delivered by an LC Star jet nebulizer, the NAC concentration in the upper airways (generations 1–10) can reach a maximum concentration of about 50 mmol/l, with the concentration exceeding 10 mmol/l for more than 1 hour. Lower doses are achieved in the small airways (C Ehre, personal communication, 2014). We found that 5 mmol/l NAC can have a large effect on AAV1 transport (**Figure 5a**,**b**; we note that the sputum samples used in the NAC study were different from the samples used in **Figures 2** and **3**, and thus the percentage of fast AAV1 particles differs between **Figures 2b** and **5a**). On average, more than 47% of the AAV1 particles diffused rapidly in NAC-treated sputum, compared with only 5% in untreated sputum. Again, we observed substantial sample-to-sample variation. In three of the five sputum samples tested, NAC improved AAV transport by one order of magnitude, whereas in two samples, NAC had little effect.

For NAC to be viable as an adjuvant for CF gene therapy, AAV must maintain its ability to transduce airway epithelial cells in the presence of NAC. We therefore assessed AAV1 transduction of BEAS-2B cells with and without 5 mmol/l NAC in the cell culture media (**Figure 5c**). We found that NAC only slightly reduced transduction (by 10%; one-sided *t*-test, $P = 0.027$). Together, our experiments indicate that NAC can increase AAV1 penetration

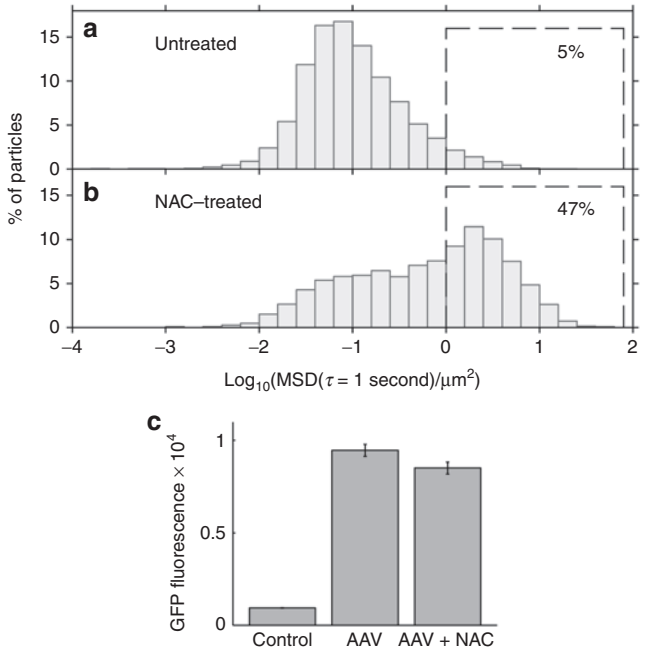

Figure 5 Effect of mucolytic agent *N*-acetylcysteine (NAC) on adeno-associated virus (AAV)1 transport in cystic fibrosis (CF) sputum and on AAV1 transduction in BEAS-2B cells. (**a–b**) Multiple particle tracking of AAV1 in CF sputum samples either (**a**) untreated or (**b**) pretreated with 5 mmol/l NAC. Graphs show distribution of individual particles' mean squared displacement (MSDs) at a time scale of 1 second. Data represent five sputum samples, with an average of >900 AAV particles tracked per sample. Percentage of particles that moved rapidly, defined as $\log_{10}$MSD ≥ 0 at a time scale of 1 second, is shown for both conditions (dashed boxes). The sputum samples used for the NAC study were different from the sputum samples used for **Figures 2** and **3**, and thus the percentage of fast AAV1 particles differs between **Figures 2b** and **5a**. (**c**) Effect of 5 mmol/l NAC in the cell culture media on AAV1 transduction of BEAS-2B cells. Results show mean cell GFP fluorescence, measured by flow cytometry, in arbitrary units. Error bars represent standard error of the mean ($P = 0.027$, $n = 8$).

through sputum at concentrations that do not dramatically affect the virus's ability to transduce cells in culture. We expect similar results for other AAV serotypes, as NAC works in a nonspecific manner by disrupting mucin crosslinking.

DISCUSSION

Here, we report that CF sputum strongly hindered the transport of clinically and preclinically tested AAV serotypes, including AAV1, 2, and 5. We estimate that only 5–15% of AAV particles can penetrate a physiologically relevant distance in sputum fast enough to avoid clearance. This finding suggests that the CF sputum barrier likely contributed to the disappointing results of AAV2 clinical trials, by preventing most of the inhaled gene vectors from reaching airway epithelial cells. The inability of AAV to efficiently penetrate sputum necessitates strategies to overcome this barrier. We discovered that modulating the adhesive interactions and steric obstruction of AAV in sputum could improve virus transport, which suggests that it may be possible to overcome the CF sputum barrier to AAV gene therapy. Our discoveries were enabled by multiple particle tracking and automated image analysis to examine tens of thousands of virus particles in >20 patient samples.

Adhesion is likely the primary mechanism by which sputum hinders AAV diffusion. There was a substantially smaller fraction of fast-moving AAV than of 100-nm PS-PEG particles—even though AAV is approximately four times smaller in diameter (~25 nm). This most likely occurred because AAV adheres to the network of biomolecules present in sputum, whereas the PEG-coated particles resist adhesion because of their inert surfaces.[10,18] Viruses may bind to sputum components nonspecifically, such as by electrostatic interactions.[31] AAV may also adhere to sputum by specific binding interactions. AAV2 binds specifically to heparan sulfate proteoglycan,[14] which is abundant in the CF lung.[27] AAV5 binds to α2,3 *N*-linked sialic acids,[15] while AAV1 binds to both α2,3 and α2,6 *N*-linked sialic acids.[16] Mucins are rich in sialic acids, though predominantly of the *O*-linked variety.[16] One study demonstrated that AAV5 did bind to purified mucin,[32] though other studies showed that AAV1 and AAV5 did not bind strongly to purified mucin.[16,33] Mucins from different sources and disease states may vary in their glycosylation, and this could explain the contradictory reports. Secondary receptors have also been identified for AAV2 and AAV5.[17] Finally, antibodies may trap AAV in sputum.[7] Because of their small size, antibodies diffuse relatively unimpeded in human mucus, but the antibody Fc region forms transient, low-affinity bonds with mucus.[34] As antibodies accumulate on the surface of a virus, multivalent antibody interactions with the mucus mesh can trap the virus.[34] Neutralizing antibodies against AAV2 have been found in ~30% of adults with CF.[35,36] Antibodies against AAV serotypes 1, 5, 6, 7, and 8 have also been found in humans, though typically with lower prevalence compared with AAV2.[36,37]

Physical obstruction by the sputum biopolymer meshwork can also trap particles. In a subset of patient samples, we found that the 100-nm PS-PEG particles, which resist adhesion to sputum, were mostly immobilized. This suggests that those samples' average pore size was less than 100 nm. Physical obstruction by the sputum meshwork likely contributed greatly to hindering AAV in those samples. Small pores also contribute to adhesive trapping, by increasing the probability of multivalent binding interactions between AAV and sputum.[10] Sputum samples can have a wide range of pore sizes,[25] so even samples with larger average pore sizes likely have some pores small enough to impede AAV motion.

We showed that modulating adhesion and physical obstruction may improve AAV diffusion in sputum. We tested a mutant AAV2, engineered at two capsid positions to have reduced heparin binding, and found that it diffused significantly faster in sputum than did AAV2. We attribute the faster transport of the mutant to reduced adhesion to heparan sulfate in sputum. A critical consideration is whether the AAV2 capsid modification will reduce transduction of polarized airway epithelial cells. Recent research shows that heparan sulfate is not essential for AAV2 transduction of airway cells,[38] so the AAV2 mutant may permit improved sputum penetration without compromising the vector's ability to transduce airway epithelial cells *in vivo*. Our work provides proof of the concept that capsid modification may be an effective strategy for improving AAV diffusion in sputum, and it motivates further research to design a gene vector that can rapidly penetrate sputum but is excellent at transducing lung cells *in vivo*. This may be a challenging task in general, given that the binding domains

of cell surface receptors necessary for AAV transduction may also be present in sputum. A high-throughput screen of many AAV mutants may be the best approach to address this challenge.

We also found that physically altering sputum using the mucolytic drug NAC, which breaks intermolecular disulfide crosslinks and depolymerizes mucins, could markedly improve AAV transport in CF sputum. For some patients, this may be a relatively simple and feasible approach for improving gene vector penetration in sputum. NAC improved AAV transport by one order of magnitude in three of five sputum samples. The two sputum samples that showed little change with NAC treatment might have had high mucin content, as we previously found that the effectiveness of NAC treatment was inversely correlated with the mucin concentration—and hence the concentration of disulfide bonds—in the sputum sample.[25] In a recent review, the CF Foundation consensus panel found insufficient evidence that NAC improved CF patients' lung function, so could not recommend for or against its routine use; in contrast, the panel did recommend use of recombinant human DNase (dornase alfa, proprietary name Pulmozyme), which acts as a mucolytic by degrading DNA in CF sputum and significantly improves pulmonary outcomes.[39] For the purposes of improving nanoparticle transport in sputum, however, our group previously found that DNase treatment alone was ineffective, while NAC treatment was effective.[22,25] Even if it is not routinely used for CF treatment, NAC could be useful as an adjuvant for AAV gene therapy. We did observe a small (~10%) reduction in AAV-mediated transduction of BEAS-2B cells when 5 mmol/l NAC was added to the cell culture media. This reduction is small considering that NAC treatment may permit 10-fold more AAV to penetrate sputum. Furthermore, we expect that this reduction will be even smaller in the airways, where mucins will compete for NAC, compared with our cell culture experiments, where the culture media did not contain mucin.

Although many of the AAV particles were immobilized in sputum, we found that a fraction of them were mobile, with substantial variation among patients. These data suggest that sputum may be a greater barrier to AAV gene delivery in some patients than in others. We observed a wide range in particle transport among patient samples, in agreement with other studies,[40] from essentially all particles immobilized to many particles diffusive. We reason that a complex interplay between patients' lung health, microbial colonization, mucin biochemistry, and airway hydration determines the physicochemical properties of their sputum, and thereby governs the extent to which their sputum sterically and adhesively impedes particle diffusion. It would be clinically useful to understand the molecular origins of these differences and identify sputum biomarkers predictive of AAV transport, but given the complex biochemistry of sputum, such an undertaking was beyond the scope of our current investigation.

We have also shown that labeling AAV with Alexa Fluor dye does not affect the virus infectivity or transport in CF sputum. Still, there are limitations to our experimental approach. The labeled viruses typically have low fluorescence intensity, and lower signal-to-noise ratio results in worse tracking resolution. More broadly, our approach of tracking viruses in expectorated sputum samples may not fully mimic the *in vivo* situation. First, the sputum that patients are able to cough out may differ somewhat in composition from the secretions coating their airways. Second, airway secretions *in vivo* sit above the cell-associated periciliary layer,[41] which may pose an additional barrier to gene delivery. However, recent work shows that the small size of AAV may facilitate penetration through the periciliary layer as well.[42] Third, while we studied the barrier properties of sputum, we did not directly assess how sputum affects AAV transduction.[12,43] One alternative experimental approach to address this issue would be to layer human CF sputum on top of cultured cells, then add AAV above the sputum, and assess how the sputum barrier affects transduction. We have found this to be challenging in practice because the CF sputum samples tend to infect the cell cultures with bacteria, and furthermore, it is difficult to add sputum at a physiologically accurate thickness (on the order of tens of micrometers). Fourth, we conducted the particle-tracking experiments in static sputum samples, whereas the CF lung is a dynamic environment with at least some ciliary activity. In future studies, it would be valuable to study the transport of promising gene vectors both in human CF sputum and in the secreted mucus layer on primary airway epithelial cells cultured at the air–liquid interface. The former material more closely mimics the secretions lining the diseased CF lung, while the latter approach would permit us to study gene vector mobility in a dynamic environment with beating cilia. Air–liquid interface cultures would enable us to experimentally compare the rate at which gene vectors can diffuse through mucus with the rate at which they are swept away by mucociliary clearance.

In summary, this work quantitatively demonstrated that CF sputum is a significant barrier to AAV gene therapy and showed that capsid modification and the mucolytic adjuvant NAC enhanced AAV diffusion in sputum. In recent years, researchers have made promising advances in overcoming various roadblocks to AAV gene therapy, including engineering the AAV capsid to increase lung transduction,[44] optimizing the viral genome to enhance CFTR expression,[6] and minimizing immune response to AAV.[3] Our findings emphasize that CF sputum is another roadblock to CF gene therapy, and we provide guidance on how to overcome the sputum barrier to achieve improved clinical outcomes.

MATERIALS AND METHODS

Production of AAV. Recombinant AAV was prepared by the Vector Core at the University of Florida Powell Gene Therapy Center. AAV1, 2, and 5 were packaged with pTR-UF11 (single-stranded enhanced GFP (eGFP) genome). For AAV1, the *rep2*, *cap1*, and AdV early genes were contained in the helper plasmid pKrap1A. For AAV2, the *rep2*, *cap2*, and AdV genes were contained in the helper plasmid pDG-KanR. For AAV5, the *rep2*, *cap5*, and AdV genes were contained in the helper plasmid pXYZ5.

The mutant AAV2 studied in this paper had the arginine residues at capsid positions 585 and 588 mutated to alanines. These mutations have previously been shown to reduce heparin binding.[14,29,30] The virus packaged pds-eGFP (double-stranded eGFP genome). The helper plasmids were pXX6 (containing the AdV genes) and mutant pIM45 (containing *rep2* and the mutant *cap2*).

AAV was produced as previously described.[45,46] Briefly, the vectors were produced via calcium phosphate-based cotransfection (for AAV1, 2, and 5) or triple transfection (for the AAV2 mutant) of plasmid into HEK293 cells. The transfected cells were incubated for ~72 hours, then harvested, and lysed by freeze/thaw. The resultant cell lysates were digested with benzonase, centrifuged to remove cellular debris, and purified by

iodixanol density step gradient centrifugation followed by ion exchange chromatography. Buffer exchange and concentration were performed using centrifugal concentrators into the final stock buffer (phosphate-buffered saline (PBS)).

AAV produced by this technique is at least 99% pure, as determined by polyacrylamide gel electrophoresis/silver stain.[47] The iodixanol density gradient centrifugation procedure separates full, genome-containing capsids from both free capsid proteins and empty capsids.[45] This was confirmed by comparing the capsid enzyme-linked immunosorbent assay titer (PROGEN Biotechnik GmbH, Heidelberg, Germany), using monoclonal antibodies that recognize only intact capsids, with the genome titer measured by DNA dot blot.

Fluorescent labeling of AAV. For virus tracking, AAV was labeled with the amine-reactive fluorescent dye Alexa Fluor 647 carboxylic acid, succinimidyl ester (AF647; Life Technologies, Carlsbad, CA). The autofluorescence of CF sputum is minimized at long-wavelength excitation, so using a deep red fluorophore such as AF647 allowed us to more easily distinguish the AAV particles. The labeling protocol was based on methods reported in the AAV literature.[48] AF647 was reconstituted in dimethyl sulfoxide and added, along with borate buffer (pH 8.3), to AAV. The final reaction volume was 150 µl and contained ~10^{11} virus particles, 15% (v/v) dimethyl sulfoxide, 100 mmol/l borate buffer, and 100 µmol/l AF647. The reaction was placed on a lab rotator at 4 °C in the dark. After 2 hours, unreacted dye molecules were removed by buffer exchange into PBS using a standard separation technique, gel filtration chromatography,[48] whereby unreacted dye was retained in the gel filtration media while labeled virus eluted from the column. The gel filtration medium we used was Sephadex G-50 (illustra ProbeQuant G-50 Micro Columns; GE Healthcare, Little Chalfont, UK). Labeled virus was stored in 5-µl aliquots at −80 °C.

Quantitative real-time polymerase chain reaction. Titers of AAV and AF647-labeled AAV were measured using quantitative real-time polymerase chain reaction on a MyiQ2 thermal cycler (Bio-Rad, Hercules, CA) using SsoAdvanced SYBR Green Supermix (Bio-Rad). Primers against the cytomegalovirus/chicken β actin promoter in the AAV genomes were purchased from Eurofins MWG Operon (Huntsville, AL) with the following sequences: forward primer, 5′-TCCCATAGTAACGCCAATAGG-3′, reverse primer, 5′-CTTGGCATATGATACACTTGATG-3′.[46] Equal numbers of viruses were then used to compare the infectivity of AAV2 and AAV2-AF647 in cell culture.

Cell transduction experiments and flow cytometry. AAV transduction experiments were conducted using a human bronchial epithelial cell line, BEAS-2B. The cells were grown in DMEM/F12 (Life Technologies) supplemented with 10% fetal bovine serum (Life Technologies) and antibiotics (100 U/ml penicillin and 100 µg/ml streptomycin; Quality Biological, Gaithersburg, MD). Cells were incubated at 37 °C in a 5% CO_2 atmosphere. For the transduction experiments, cells were seeded at a density of 40,000 cells/well in 24-well plates. After seeding, cells were allowed to grow for 24 hours before adding AAV.

For comparing the infectivity of AAV2 with AF647-labeled AAV2, virus was added to the cells at a multiplicity of infection of 2×10^3 vgc/cell. GFP expression was measured by flow cytometry 48 hours after adding the virus.

We conducted heparin competition experiments to check the relative heparin binding strengths of AAV2 and the AAV2 mutant. In these studies, prior to the addition of virus, the regular medium was replaced with medium into which had been dissolved heparin sodium salt (from porcine intestinal mucosa; Sigma-Aldrich, St Louis, MO) at concentrations of 10, 25, or 100 µg/ml. A multiplicity of infection of 10^5 vgc/cell was used throughout, to achieve significant GFP expression for all serotypes, including the AAV2 mutant, which generally has lower transduction efficiency than wild-type AAV2 *in vitro*.[14] The medium was removed 3 hours after adding the virus and replaced with fresh medium without heparin. GFP expression was measured by flow cytometry 48 hours after adding the virus.

To determine whether NAC affected AAV1 transduction, we conducted experiments in which, immediately prior to adding virus, the regular cell culture medium was replaced with medium containing NAC at a concentration of 5 mmol/l. AAV1 was then added at a multiplicity of infection of 2×10^4 vgc/cell. GFP expression was measured by flow cytometry 48 hours after adding the virus.

Flow cytometry was conducted with an Accuri C6 flow cytometer (BD Biosciences, San Jose, CA) using the 488-nm laser. GFP fluorescence was detected in the FL1 channel with a 533/30-nm band-pass filter. For each well on a 24-well plate, 10,000 cells were counted.

CF sputum sample collection. Expectorated sputum samples were collected from patients at the adult CF clinics at Johns Hopkins ($n = 23$) and the University of Alabama at Birmingham ($n = 3$). Samples from Hopkins were stored at 4 °C and analyzed the day after collection. Samples from Alabama were shipped overnight, on ice, to Hopkins and also analyzed the day after sample collection. Samples were collected under written informed consent, in accordance with Institutional Review Board approval and following Declaration of Helsinki protocols.

Patients involved in this study received no mucolytics other than Pulmozyme as part of their treatment regimen. Nineteen percent of the patients received Pulmozyme between 2 and 6 hours prior to their sputum sample collection, 50% of patients last received Pulmozyme the day before sample collection or earlier, and 31% of patients were not taking Pulmozyme.

Preparing PS-PEG and PS-PEG-AF647 nanoparticles. PEG-coated PS particles (PS-PEG) were prepared as detailed previously.[10] Briefly, fluorescent carboxylate-modified PS spheres (PS-COOH), 100 and 500 nm in diameter, were purchased from Life Technologies or Bangs Laboratories (Fishers, IN). To coat the PS-COOH particles with PEG, 5 kDa methoxy-PEG-amine (Creative PEGWorks, Winston-Salem, NC) was covalently coupled to carboxyl groups on the PS-COOH particles using 1-ethyl-3-(3-dimethylaminopropyl) carbodiimide hydrochloride (EDC) and N-hydroxysulfosuccinimide sodium salt (sulfo-NHS; Sigma-Aldrich) in borate buffer (pH 8.3). After reacting for 4 hours, the resulting PS-PEG particles were centrifuged and washed in ultrapure water. Our lab recently measured the surface density of PEG on PS-PEG particles prepared according to this protocol to be 0.09 PEG/nm^2, which suggests the PEG layer has a dense brush conformation ideal for resisting protein adhesion.[49] We did not use AAV-sized polymeric particles in this paper because commercially available 20-nm PS-COOH particles are more challenging to PEGylate, and they also have lower fluorescence intensity and consequently are more difficult to track, compared with 100-nm or larger PS-COOH particles.

To prepare 100-nm PS-PEG particles labeled with AF647 (PS-PEG-AF647), a modified version of this protocol was used. First, the carboxyl groups on the PS-COOH particles were activated by reacting PS-COOH particles, NHS, and EDC in 50 mmol/l MES buffer (pH 6.0) for 1 hour. Next, the particles were centrifuged and resuspended in 100 mmol/l borate buffer (pH 8.3), to which 5 kDa carboxyl-PEG-amine (JenKem Technology USA, Allen, TX) was added at a fivefold molar excess to the number of carboxyl groups on the PS-COOH particles. This mixture was allowed to react for 2 hours, to couple the amine groups on the PEG with the activated carboxyl groups on the particles. Then, the particles were centrifuged and resuspended in fresh borate buffer, to which was added NHS, EDC, and Alexa Fluor 647 cadaverine, disodium salt (Life Technologies). The dye was added at a 1:1 molar ratio to the number of carboxyl groups on the PS-COOH particles (the maximum number of PEG chains that could have attached). This mixture reacted overnight, coupling the amine on the AF647-cadaverine with the carboxyl group on the free end of the PEG chains. Finally, the PS-PEG-AF647 particles were

centrifuged and washed in ultrapure water until the supernatant was free of visible dye.

PS-COOH, PS-PEG, and PS-PEG-AF647 particles were stored at 4 °C. For particle-tracking experiments, the particles were diluted with ultrapure water to concentrations ideal for tracking individual particles.

Particle size measurements. AAV and nanoparticle size were measured by dynamic light scattering using a Zetasizer Nano ZS (Malvern Instruments, Malvern, UK), which uses a 633-nm laser and has a 173° scattering angle. Measurements were conducted at 25 °C. AAV was suspended in PBS (pH 7.4), while the nanoparticles were suspended in PBS diluted to have a 10 mmol/l NaCl concentration.

Scanning electron microscopy. Sputum was prepared for electron microscopy following an established protocol, as described previously.[10] Briefly, sputum samples were fixed in 2% glutaraldehyde, postfixed in 1% OsO_4, and then stained with 2% uranyl acetate. The specimens were then dehydrated through a graded series of ethanol solutions, followed by immersion in hexamethyldisilazane, and then desiccated under vacuum overnight. The samples were attached to aluminum stub mounts, sputter coated with 20-nm of AuPd, and imaged with a field-emission scanning electron microscope (LEO 1530 FESEM; Zeiss, Jena, Germany).

Particle tracking: sample preparation and microscopy. Movement of viruses and nanoparticles in sputum was measured by multiple particle tracking. The sample preparation procedure was designed to minimize manipulation of the sputum and maintain its microarchitecture. Sputum aliquots (~30 µl each) were withdrawn from the sputum sample using a Wiretrol (Drummond Scientific Company, Broomall, PA) and dispensed into custom microscopy chambers. Aliquots were withdrawn from the same approximate location in the sputum sample to minimize the effects of intrasample heterogeneity.

To each sputum aliquot was added 0.5 µl of one serotype of AF647-labeled AAV, plus polymeric nanoparticles as controls: 0.5 µl of green fluorescent 500-nm PS-PEG particles, 0.5 µl of red fluorescent 100-nm PS-PEG particles, or 0.5 µl each of the 100-nm and 500-nm PS-PEG particles. Thus, in total, no more than 1.5 µl of virus and nanoparticle suspensions were added to ~30 µl of sputum, so the sputum aliquots were diluted 5% v/v or less. In our current and previously published work, we found that dilutions of this magnitude did not alter the ability of sputum to sterically and adhesively trap particles.[18,25]

After adding the particles, the sputum aliquots were gently stirred with a pipette tip, and then the chambers were sealed with a coverslip to prevent sample dehydration. After incubating the chambers for 1 hour, they were imaged at room temperature using an inverted epifluorescence microscope (Axio Observer; Zeiss) located on a vibration isolation table and employing a ×100/1.46 NA oil-immersion objective. Care was taken to focus the objective at least 2 µm away from the coverslip to minimize edge effects. Movies of virus and nanoparticle motion in the sputum samples were recorded at a frame rate of 15 Hz, for 150 or 300 frames, using an EM-CCD camera (Evolve 512; Photometrics, Tuscon, AZ). For each sputum sample, 5–10 movies of each virus serotype or nanoparticle type were collected.

To determine the effect of the mucolytic drug NAC on AAV transport in CF sputum, a solution of NAC (neutralized to a pH of 7) was mixed into sputum to a final concentration of 5 mmol/l. For the untreated control, a comparable volume of PBS was added to sputum. NAC-treated and control samples were then incubated at 37 °C for 30 minutes. AAV1-AF647 was then added to the samples in custom microscopy chambers, the slides were incubated for 1 hour at 37 °C, and imaging was performed using the procedure above. In this experiment, the sputum samples were again diluted 5% (v/v) or less. Finally, to determine the effect of AF647 labeling on particle transport, we prepared sputum aliquots with 100-nm PS-PEG, 100-nm PS-PEG-AF647, and 100-nm PS-COOH particles.

Particle-tracking analysis. Movies were analyzed using automated particle-tracking software custom-written in MATLAB (MathWorks, Natick, MA), based on the algorithm of Crocker and Grier,[21] to determine the x and y positions of particles over time. Images were first processed by convolving them with a spatial bandpass filter to reduce noise and nonuniform background. Local maxima of pixel intensity were identified as candidate particle positions. These positions were refined by calculating the intensity-weighted centroid of the bright spots, to yield subpixel resolution. By examining particle brightness, size, and eccentricity, true particles were retained and spurious ones (noise) discarded. Trajectories were constructed by linking particle positions identified in subsequent frames via a nearest neighbor method. Trajectories shorter than 1 second were discarded. The time-averaged mean squared displacement (MSD) of each trajectory was calculated as $MSD(\tau) = \langle[x(t+\tau) - x(t)]^2\rangle + \langle[y(t+\tau) - y(t)]^2\rangle$, where τ is the time scale and the angled brackets denote the average over many starting times t. Scanning electron microscopy (**Supplementary Figure S1**) suggests that sputum is isotropic, so the two-dimensional MSD measured here equals two-thirds of the three-dimensional MSD.

Tracking resolution was estimated based on a published method.[50] First, the signal-to-noise ratio was calculated from the experimental movies (particle-tracking movies of AAV and nanoparticles in sputum). These were compared with a standard curve of static error as a function of signal-to-noise ratio, to estimate the static error in the experimental movies. The standard curve was generated by affixing particles to a glass slide and tracking them under different illumination intensities; the apparent motion of these fixed particles is due to static error. For 100-nm PS-PEG particles in sputum, the tracking resolution was ~25 nm. For AAV, the tracking resolution was ~75 nm, since the viruses are dim and their positions cannot be estimated as accurately. The MSDs of fast particles and viruses—those of greatest clinical interest, because they are most likely to penetrate CF sputum—are well above the noise floor at a time scale of 1 second.

Statistical analysis. Student's t-tests and analysis of variance were conducted in MATLAB (MathWorks). Linear mixed-effects models were constructed using the lme4 package[24] in the statistical language R to examine the relationship between AAV2 capsid and MSD (at a time scale of 1 second) in sputum. In these models, MSD was the dependent variable, and AAV2 capsid (mutated or wild-type) was set as a fixed effect. The random effects were patient sample number, as well as by-patient random slopes for the effect of AAV capsid. Residual plots did not show major deviations from homoscedasticity or normality. The p value was calculated by a likelihood ratio test of the full model, which includes AAV capsid type, against the null model, which excludes AAV capsid type. Linear mixed-effects models were also used to compare the extent of intra- and intersample variability; here, MSD of 100-nm PS-PEG particles was the dependent variable and both patient and sputum aliquot numbers were set as random effects.

SUPPLEMENTARY MATERIAL

Figure S1. Scanning electron micrograph of CF sputum.
Figure S2. Transport of polymeric nanoparticles in CF sputum.
Figure S3. Diffusion of AAV in water.
Figure S4. Intra- and intersputum sample heterogeneity.
Figure S5. Heparin-binding assay.

ACKNOWLEDGMENTS

This work was supported by the National Institutes of Health (grant P01HL51811) and the Cystic Fibrosis Foundation (HANES07XX0 and ROWE10XX0). We thank Meagan Ramsey and the entire staff of the Johns Hopkins Adult Cystic Fibrosis Clinic for collecting patient sputum samples and Erin Tallarico for compiling patient demographic data. We thank Maxim Salganik and Mark Potter (University of Florida) for advice on AAV; Kah Suan Lim (Johns Hopkins) for help with polymerase chain reaction; Jennifer Feder Bobb (Harvard School of Public Health) for

assistance with statistics; and Jane Chisholm, Liudmila Cebotaru, Craig Schneider, Laura Ensign, Panagiotis Mastorakos, and Tao Yu (Johns Hopkins) for helpful discussions. We thank the Johns Hopkins School of Medicine Microscope Facility staff for assistance with scanning electron microscopy and advice on particle tracking. N.M. is an inventor of patents related to recombinant AAV technology and owns equity in a company that is commercializing AAV for gene therapy applications.

REFERENCES

1. Sosnay, PR, Siklosi, KR, Van Goor, F, Kaniecki, K, Yu, H, Sharma, N *et al.* (2013). Defining the disease liability of variants in the cystic fibrosis transmembrane conductance regulator gene. *Nat Genet* **45**: 1160–1167.
2. O'Sullivan, BP and Freedman, SD (2009). Cystic fibrosis. *Lancet* **373**: 1891–1904.
3. Griesenbach, U and Alton, EW (2012). Progress in gene and cell therapy for cystic fibrosis lung disease. *Curr Pharm Des* **18**: 642–662.
4. Johnson, LG, Boyles, SE, Wilson, J and Boucher, RC (1995). Normalization of raised sodium absorption and raised calcium-mediated chloride secretion by adenovirus-mediated expression of cystic fibrosis transmembrane conductance regulator in primary human cystic fibrosis airway epithelial cells. *J Clin Invest* **95**: 1377–1382.
5. Hyde, SC, Gill, DR, Higgins, CF, Trezise, AE, MacVinish, LJ, Cuthbert, AW *et al.* (1993). Correction of the ion transport defect in cystic fibrosis transgenic mice by gene therapy. *Nature* **362**: 250–255.
6. Mueller, C and Flotte, TR (2008). Gene therapy for cystic fibrosis. *Clin Rev Allergy Immunol* **35**: 164–178.
7. Sanders, N, Rudolph, C, Braeckmans, K, De Smedt, SC and Demeester, J (2009). Extracellular barriers in respiratory gene therapy. *Adv Drug Deliv Rev* **61**: 115–127.
8. Flotte, TR, Fischer, AC, Goetzmann, J, Mueller, C, Cebotaru, L, Yan, Z *et al.* (2010). Dual reporter comparative indexing of rAAV pseudotyped vectors in chimpanzee airway. *Mol Ther* **18**: 594–600.
9. Fahy, JV and Dickey, BF (2010). Airway mucus function and dysfunction. *N Engl J Med* **363**: 2233–2247.
10. Schuster, BS, Suk, JS, Woodworth, GF and Hanes, J (2013). Nanoparticle diffusion in respiratory mucus from humans without lung disease. *Biomaterials* **34**: 3439–3446.
11. Hida, K, Lai, SK, Suk, JS, Won, SY, Boyle, MP and Hanes, J (2011). Common gene therapy viral vectors do not efficiently penetrate sputum from cystic fibrosis patients. *PLoS One* **6**: e19919.
12. Kitson, C, Angel, B, Judd, D, Rothery, S, Severs, NJ, Dewar, A *et al.* (1999). The extra- and intracellular barriers to lipid and adenovirus-mediated pulmonary gene transfer in native sheep airway epithelium. *Gene Ther* **6**: 534–546.
13. Liu, X, Yan, Z, Luo, M and Engelhardt, JF (2006). Species-specific differences in mouse and human airway epithelial biology of recombinant adeno-associated virus transduction. *Am J Respir Cell Mol Biol* **34**: 56–64.
14. Opie, SR, Warrington, KH Jr, Agbandje-McKenna, M, Zolotukhin, S and Muzyczka, N (2003). Identification of amino acid residues in the capsid proteins of adeno-associated virus type 2 that contribute to heparan sulfate proteoglycan binding. *J Virol* **77**: 6995–7006.
15. Walters, RW, Yi, SM, Keshavjee, S, Brown, KE, Welsh, MJ, Chiorini, JA *et al.* (2001). Binding of adeno-associated virus type 5 to 2,3-linked sialic acid is required for gene transfer. *J Biol Chem* **276**: 20610–20616.
16. Wu, Z, Miller, E, Agbandje-McKenna, M and Samulski, RJ (2006). Alpha2,3 and alpha2,6 N-linked sialic acids facilitate efficient binding and transduction by adeno-associated virus types 1 and 6. *J Virol* **80**: 9093–9103.
17. Asokan, A, Schaffer, DV and Samulski, RJ (2012). The AAV vector toolkit: poised at the clinical crossroads. *Mol Ther* **20**: 699–708.
18. Suk, JS, Lai, SK, Wang, YY, Ensign, LM, Zeitlin, PL, Boyle, MP *et al.* (2009). The penetration of fresh undiluted sputum expectorated by cystic fibrosis patients by non-adhesive polymer nanoparticles. *Biomaterials* **30**: 2591–2597.
19. Kim, AJ, Boylan, NJ, Suk, JS, Hwangbo, M, Yu, T, Schuster, BS *et al.* (2013). Use of single-site-functionalized PEG dendrons to prepare gene vectors that penetrate human mucus barriers. *Angew Chem Int Ed Engl* **52**: 3985–3988.
20. Berg, HC (1993). *Random Walks in Biology*. Princeton University Press: Princeton, NJ, pp. 152.
21. Crocker, JC and Grier, DG (1996). Methods of digital video microscopy for colloidal studies. *J Colloid Interface Sci* **179**: 298–310.
22. Dawson, M, Wirtz, D and Hanes, J (2003). Enhanced viscoelasticity of human cystic fibrotic sputum correlates with increasing microheterogeneity in particle transport. *J Biol Chem* **278**: 50393–50401.
23. Hamid, Q, Shannon, J and Martin, JG (2005). *Physiologic Basis of Respiratory Disease*. BC Decker: Hamilton, ON, pp. 793.
24. Bates, D, Maechler, M, Bolker, B and Walker, S (2014). lme4: Linear mixed-effects models using Eigen and S4.R package version 1.1-6. http://CRAN.R-project.org/package=lme4.
25. Suk, JS, Boylan, NJ, Trehan, K, Tang, BC, Schneider, CS, Lin, JM *et al.* (2011). N-acetylcysteine enhances cystic fibrosis sputum penetration and airway gene transfer by highly compacted DNA nanoparticles. *Mol Ther* **19**: 1981–1989.
26. Suk, JS, Lai, SK, Boylan, NJ, Dawson, MR, Boyle, MP and Hanes, J (2011). Rapid transport of muco-inert nanoparticles in cystic fibrosis sputum treated with N-acetyl cysteine. *Nanomedicine (Lond)* **6**: 365–375.
27. Solic, N, Wilson, J, Wilson, SJ and Shute, JK (2005). Endothelial activation and increased heparan sulfate expression in cystic fibrosis. *Am J Respir Crit Care Med* **172**: 892–898.
28. Chan, SC, Shum, DK and Ip, MS (2003). Sputum sol neutrophil elastase activity in bronchiectasis: differential modulation by syndecan-1. *Am J Respir Crit Care Med* **168**: 192–198.
29. Wu, P, Xiao, W, Conlon, T, Hughes, J, Agbandje-McKenna, M, Ferkol, T *et al.* (2000). Mutational analysis of the adeno-associated virus type 2 (AAV2) capsid gene and construction of AAV2 vectors with altered tropism. *J Virol* **74**: 8635–8647.
30. Kern, A, Schmidt, K, Leder, C, Müller, OJ, Wobus, CE, Bettinger, K *et al.* (2003). Identification of a heparin-binding motif on adeno-associated virus type 2 capsids. *J Virol* **77**: 11072–11081.
31. Lieleg, O, Lieleg, C, Bloom, J, Buck, CB and Ribbeck, K (2012). Mucin biopolymers as broad-spectrum antiviral agents. *Biomacromolecules* **13**: 1724–1732.
32. Auricchio, A, O'Connor, E, Hildinger, M and Wilson, JM (2001). A single-step affinity column for purification of serotype-5 based adeno-associated viral vectors. *Mol Ther* **4**: 372–374.
33. Walters, RW, Pilewski, JM, Chiorini, JA and Zabner, J (2002). Secreted and transmembrane mucins inhibit gene transfer with AAV4 more efficiently than AAV5. *J Biol Chem* **277**: 23709–23713.
34. Wang, YY, Kannan, A, Nunn, KL, Murphy, MA, Subramani, DB, Moench, T *et al.* (2014). IgG in cervicovaginal mucus traps HSV and prevents vaginal Herpes infections. *Mucosal Immunol* doi: 10.1038/mi.2013.120 (e-pub ahead of print).
35. Chirmule, N, Propert, K, Magosin, S, Qian, Y, Qian, R and Wilson, J (1999). Immune responses to adenovirus and adeno-associated virus in humans. *Gene Ther* **6**: 1574–1583.
36. Halbert, CL, Miller, AD, McNamara, S, Emerson, J, Gibson, RL, Ramsey, B *et al.* (2006). Prevalence of neutralizing antibodies against adeno-associated virus (AAV) types 2, 5, and 6 in cystic fibrosis and normal populations: Implications for gene therapy using AAV vectors. *Hum Gene Ther* **17**: 440–447.
37. Calcedo, R, Vandenberghe, LH, Gao, G, Lin, J and Wilson, JM (2009). Worldwide epidemiology of neutralizing antibodies to adeno-associated viruses. *J Infect Dis* **199**: 381–390.
38. Boyle, MP, Enke, RA, Reynolds, JB, Mogayzel, PJ Jr, Guggino, WB and Zeitlin, PL (2006). Membrane-associated heparan sulfate is not required for rAAV-2 infection of human respiratory epithelia. *Virol J* **3**: 29.
39. Mogayzel, PJ Jr, Naureckas, ET, Robinson, KA, Mueller, G, Hadjiliadis, D, Hoag, JB *et al.* Pulmonary Clinical Practice Guidelines Committee. (2013). Cystic fibrosis pulmonary guidelines. Chronic medications for maintenance of lung health. *Am J Respir Crit Care Med* **187**: 680–689.
40. Forier, K, Messiaen, AS, Raemdonck, K, Deschout, H, Rejman, J, De Baets, F *et al.* (2013). Transport of nanoparticles in cystic fibrosis sputum and bacterial biofilms by single-particle tracking microscopy. *Nanomedicine (Lond)* **8**: 935–949.
41. Button, B, Cai, LH, Ehre, C, Kesimer, M, Hill, DB, Sheehan, JK *et al.* (2012). A periciliary brush promotes the lung health by separating the mucus layer from airway epithelia. *Science* **337**: 937–941.
42. Kesimer, M, Ehre, C, Burns, KA, Davis, CW, Sheehan, JK and Pickles, RJ (2013). Molecular organization of the mucins and glycocalyx underlying mucus transport over mucosal surfaces of the airways. *Mucosal Immunol* **6**: 379–392.
43. Virella-Lowell, I, Poirier, A, Chesnut, KA, Brantly, M and Flotte, TR (2000). Inhibition of recombinant adeno-associated virus (rAAV) transduction by bronchial secretions from cystic fibrosis patients. *Gene Ther* **7**: 1783–1789.
44. Excoffon, KJ, Koerber, JT, Dickey, DD, Murtha, M, Keshavjee, S, Kaspar, BK *et al.* (2009). Directed evolution of adeno-associated virus to an infectious respiratory virus. *Proc Natl Acad Sci USA* **106**: 3865–3870.
45. Zolotukhin, S, Potter, M, Zolotukhin, I, Sakai, Y, Loiler, S, Fraites, TJ Jr *et al.* (2002). Production and purification of serotype 1, 2, and 5 recombinant adeno-associated viral vectors. *Methods* **28**: 158–167.
46. Salganik, M, Aydemir, F, Nam, HJ, McKenna, R, Agbandje-McKenna, M and Muzyczka, N (2014). Adeno-associated virus capsid proteins may play a role in transcription and second-strand synthesis of recombinant genomes. *J Virol* **88**: 1071–1079.
47. Zolotukhin, S, Byrne, BJ, Mason, E, Zolotukhin, I, Potter, M, Chesnut, K *et al.* (1999). Recombinant adeno-associated virus purification using novel methods improves infectious titer and yield. *Gene Ther* **6**: 973–985.
48. Bartlett, JS, Wilcher, R and Samulski, RJ (2000). Infectious entry pathway of adeno-associated virus and adeno-associated virus vectors. *J Virol* **74**: 2777–2785.
49. Nance, EA, Woodworth, GF, Sailor, KA, Shih, TY, Xu, Q, Swaminathan, G *et al.* (2012). A dense poly(ethylene glycol) coating improves penetration of large polymeric nanoparticles within brain tissue. *Sci Transl Med* **4**: 149ra119.
50. Savin, T and Doyle, PS (2005). Static and dynamic errors in particle tracking microrheology. *Biophys J* **88**: 623–638.